Sensors and Materials, Vol. 35, No. 10 (2023) 4789–4796
MYU Tokyo

S & M 3431

Redox Cycling in Microgap Monolayer Graphene Electrodes Made without Using a Microfabrication Process

Satomi Onuki and Yuko Ueno*

Department of Applied Chemistry, Faculty of Science and Engineering, Chuo University
1-13-27 Kasuga, Bunkyo-ku, Tokyo 112-8551, Japan

(Received July 1, 2023; accepted September 13, 2023)

Keywords: monolayer graphene, microgap electrodes, redox cycling

We successfully fabricated a pair of microgap monolayer graphene electrodes (MMGEs), in which the basal planes of two monolayer graphenes are arranged in parallel facing each other across a small gap of 20 μm, without using a microfabrication process. We measured the redox cycling in the MMGEs using (ferrocenylmethyl) trimethylammonium bromide and observed an excellent redox cycling under low-speed scanning conditions of 0.005 V/s. The collection efficiency reached 97% and was almost independent of the scan rate.

1. Introduction

Monolayer graphene (MG) has attracted attention as an electrode material for biosensors owing to its excellent electrical conductivity, chemical and thermal stabilities, and high biocompatibility.[1–3] On the other hand, electrochemical biosensors require high sensitivity and selectivity to detect low-concentration molecules/ions in sample solutions. The repeated redox cycling in the small gaps in micro- and nanoscales between two working electrodes enabled sensitive electrochemical detection. Many studies have been conducted on electrodes providing planar small gaps such as interdigitated arrays,[4–9] ring-like devices,[10] and vertical gaps,[11–14] which enable a large signal amplification via redox cycling. There are many variations in electrode shape and material, and the fields of application range from basic research to cell analysis. However, to the best of our knowledge, there are few studies on the fabrication of small-gap electrodes using MG as an electrode material. The reason is that the microfabrication of MG is more difficult than that of other electrode materials, and durability in repeated measurements is also low. Since MG has an ultrathin structure consisting of a single atomic layer, it is easily removed from the substrate during the fabrication process and repeated measurements, which easily worsen the electrode properties. To overcome this problem, we have developed a fabrication process to avoid damage to the chemical vapor deposition (CVD)-grown MG as much as possible during the manufacturing of MG-based microdevices.[15] Moreover, MG is composed of edges and basal planes, and the electrochemical activity of an edge is several orders of magnitude higher than that of the basal surface.[16,17] When we use a microfabrication

*Corresponding author: e-mail: yuko.ueno.15p@g.chuo-u.ac.jp
https://doi.org/10.18494/SAM4566

ISSN 0914-4935
https://myukk.org/

process to obtain a microstructure of MG, graphene can be masked with a photoresist and dry-etched with oxygen plasma. In that case, the outline of the completed microstructure is composed of MG edges. Therefore, the electrochemical properties of the basal planes are hidden by the highly active edges and are difficult to investigate.

In this study, we successfully fabricated a pair of electrodes in which the basal planes of two MGs are arranged in parallel facing each other across a small gap of 20 μm (microgap monolayer graphene electrodes, MMGEs). Our MMGE fabrication procedure is very simple and has a large advantage, that is, we use no microfabrication process that requires special equipment and facilities. We then evaluated the basic redox cycling in the MMGEs using (ferrocenylmethyl) trimethylammonium bromide (FcTAB), which is a representative redox species in aqueous solution.

2. Materials and Methods

2.1 Reagents and chemicals

CVD-grown MG on Cu foil was purchased from Graphene Platform Corporation (Tokyo, Japan). FcTAB and 1-pyrenebutanoic acid-succinimidyl ester (Py-linker) were purchased from Tokyo Chemical Industry Co., Ltd. *N*,*N*-dimethylformamide (DMF), ethanol, and acetone were purchased from Kanto Chemical Co., Inc. Potassium chloride and 40 wt% $FeCl_3$ solution were purchased from FUJIFILM Wako Pure Chemical Corporation. 3-Aminopropyltriethoxysilane (APTES, Shin-Etsu Chemical Co., Ltd.) and polymethyl methacrylate (PMMA) solution (495 PMMA Series Resists in Anisole, A6, EM Resist Ltd.) were used as received. For electrochemical measurements, 1 mM FcTAB in 1 M KCl aqueous solution was prepared. DI water (Millipore, >18 MΩ·cm) was used in all experiments.

2.2 Fabrication of MMGE

Figure 1 shows the fabrication procedures for an MG electrode (MGE) and the MMGEs that we used in this study. We first formed an approximately 100-nm-thick Au film pattern as a device connection pad on a glass plate [slide glass (No. 2), cut into 2.6 × 1.1 cm^2, Matsunami Glass Ind., Ltd.] [Fig. 1(a)]. The patterning was performed by covering all areas other than the pad with a masking sheet. We then carried out the oxygen plasma treatment of the glass plate with metal pads to make the SiO_2 surface hydrophilic. To modify the SiO_2 surface with amine groups, we immersed the entire plate in 0.1% APTES solution dissolved in a 20:1 volume ratio mixture of ethanol and DI water for >1 h at room temperature, rinsed it with ethanol, and then dried it in a nitrogen stream [Fig. 1(b)]. The glass was then covered with a drop of 5 mM DMF solution of Py-linker for 1 h at room temperature, rinsed with DMF, and dried in a nitrogen stream. In this process, the amine group was bonded to the Py-linker by a dehydration reaction, and thus the pyrene group was immobilized on the surface of the plate [Fig. 1(c)]. Because pyrene adsorbs firmly onto the graphene surface via π–π interactions, the pyrene-modified surface works as an excellent adhesive layer for graphene.[15] Subsequently, we transferred MG

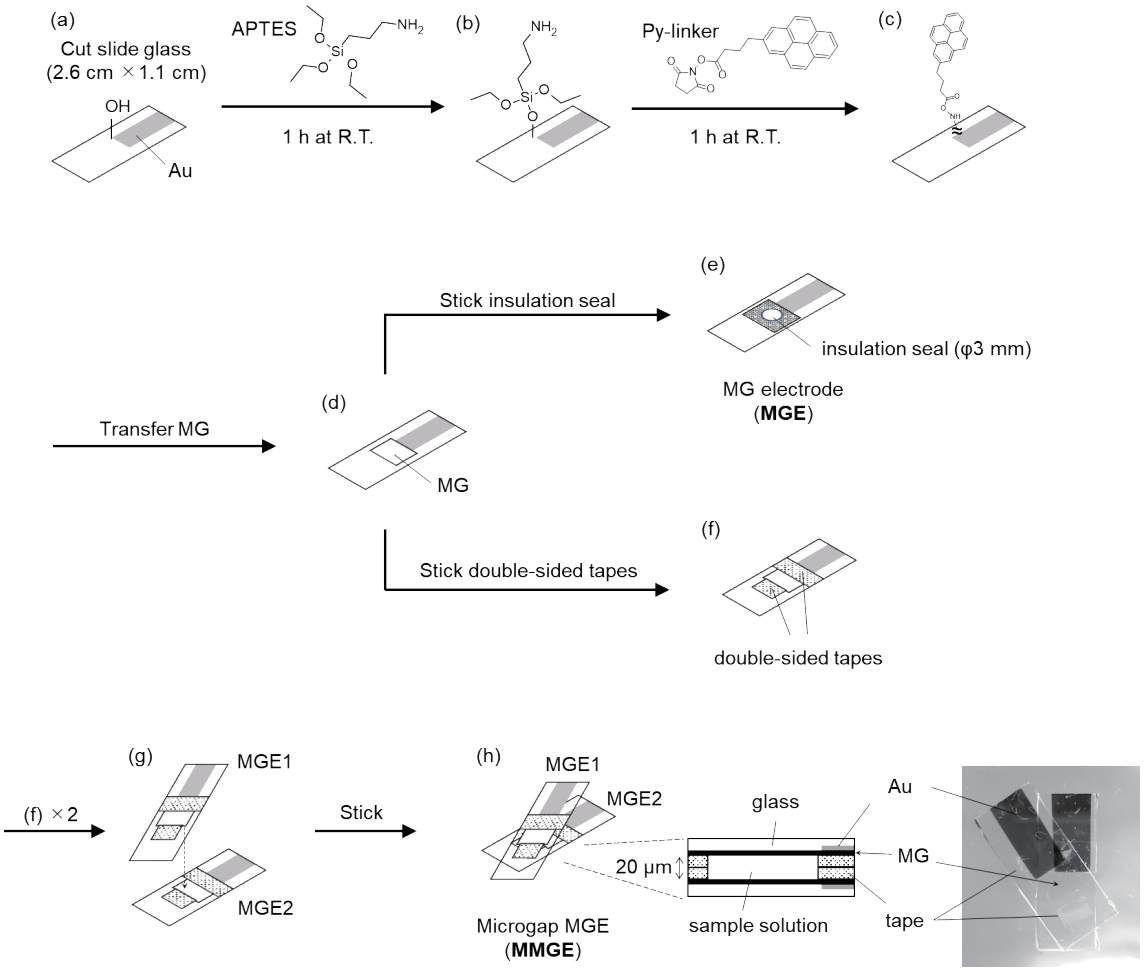

Fig. 1. Fabrication of MGE [(a) to (e)], followed by fabrication of MMGE [(f) to (g)], and cross section [(h), left] and photograph of MMGE [(h), right].

onto the plate in the same way as previously reported for the preparation of a graphene biosensor [Fig. 1(d)].[15,18] In brief, the CVD-grown MG on Cu foil was cut into pieces of the required size. The graphene surface was covered with PMMA by spin-coating. The piece was floated on $FeCl_3$ solution for approximately 1 h for Cu etching. $FeCl_3$ was replaced with DI water to wash the bottom surface of graphene with a PMMA top layer. The graphene floating on the water was then transferred onto the pyrene-modified surface of the plate. The PMMA film was removed in hot acetone, rinsed with ethanol, and air-dried. We stuck an insulation seal with a circular hole of 3 mm diameter on the MG layer to the surface of the MG and obtained an MGE [Fig. 1(e)]. We made two identical MGEs (MGE1 and MGE2) according to the above process. Then, we stuck a double-sided tape of 10 μm thickness to cover the boundary of the Au pad and the MG layer to insulate the electrode area and the pad, and the other side of the electrode [Fig. 1(f)]. Finally, we stuck MGE1 and MGE2 arranged in parallel facing each other [Fig. 1(g)]. The gap between MGE1 and MGE2 was approximately 20 μm, which was equivalent to the thickness of two

sheets of the double-sided tape [Fig. 1(h), cross section, left]. Here, we put the Au pads so as not to overlap to connect MGE1 and MGE2 independently to the electrochemical analyzer [Fig. 1(h), photograph, right]. We confirmed that the surface of the electrode was the basal plane of MG by measuring the Raman spectrum (Fig. 2).

2.3 Electrochemical analysis

Cyclic voltammetry (CV) experiments were carried out on an ALS1200C bipotentiostat (CH Instruments, Inc.) with a glass cell (Fig. 3). The sample solution was delivered between the MMGEs by spontaneous permeation through a small discontinuity of the double-sided tape. A Pt wire and a Ag/AgCl (3 M NaCl) electrode (BAS, Inc.) were used as counter and reference electrodes, respectively. A CV measurement in single mode was conducted using either MGE1 or MGE2 by cycling the potential at 0.2 to 0.6 V vs the Ag/AgCl range without using the other MGE. The scan rate was 0.05 V/s. CVs in dual mode were conducted by cycling the potential of

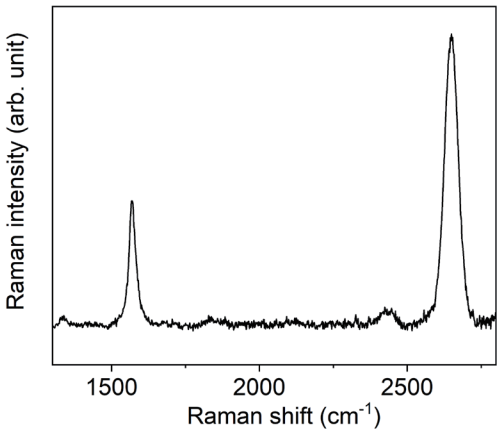

Fig. 2. Raman spectrum of MG transferred on the substrate.

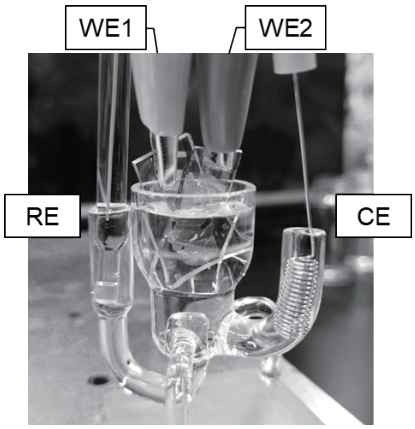

Fig. 3. Photograph of electrochemical measurement setup.

the generator electrode at 0.2 to 0.6 V vs the Ag/AgCl range while setting the potential of the collector electrode at 0.0 V vs Ag/AgCl. The scan rates were varied from 0.005 to 0.1 V/s. All the measurements were performed at room temperature.

3. Results and Discussion

3.1 Single-mode CV property

We measured the single-mode CVs of $[FcTAB]^{0/+}$ (1 mM in 1 M KCl) by using MGE1 and a circular MGE as a reference (Fig. 4). The oxidation and reduction peaks are clearly observed for both MGE1 and MGE. However, the current response at 0.6 V was approximately 0 μA for MGE1, whereas that for MGE was 4.2 μA. The difference was that the MGE1 measurement solution was confined in a narrow space, whereas the MGE measurement solution was an open system. In narrow confined spaces, the redox compound is rapidly consumed during electrochemical detection owing to the low mass transfer efficiency to the electrode surface.[19] This also occurred in MGE1 and could be explained by the rapid consumption of almost all $[FcTAB]^0$ or $[FcTAB]^+$ during the electrochemical process at MGE1. The potential differences between the oxidation and reduction peaks ($\Delta E = E_{p\_ox} - E_{p\_red}$) were 0.07 and 0.11 V with MGE1 and MGE, respectively. The results indicated that the redox reaction of $[FcTAB]^{0/+}$ on MGE is nearly quasi-reversible and can be regarded as almost diffusion-limited. The surfaces of MGE1 and MGE were both MG, and the reason why ΔE was smaller for MGE1 than for MGE cannot be described by the difference in charge transfer rate. Since MGE1 is a system with low mass transport efficiency as we described above, the redox compounds behave similarly to analyte-immobilized electrodes. Therefore, it can be explained that ΔE became smaller for MGE1 than for MGE.

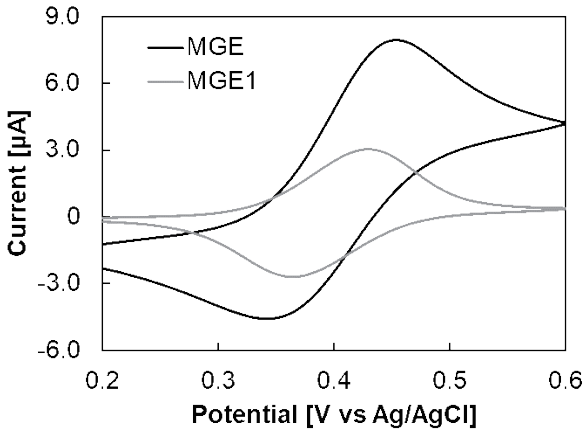

Fig. 4. Voltammograms of $[FcTAB]^{0/+}$ (1 mM in 1 M KCl) obtained with a circular MGE of 3 mm diameter (black) and MGE1 (gray). The upward and downward currents indicate the oxidation of $[FcTAB]^0$ to $[FcTAB]^+$ and the reduction of $[FcTAB]^+$ to $[FcTAB]^0$ responses, respectively.

3.2 Dual-mode CV properties of MMGEs

Next, we measured the dual-mode CVs of $[FcTAB]^{0/+}$ (1 mM in 1 M KCl) by using MGE1 and MGE2 as generator and collector electrodes, respectively (Fig. 5). Under high-speed scanning conditions of 0.1 and 0.05 V/s, the CV curve of the generator electrode resembled that of the single-mode CV, namely, both oxidation and reduction peaks were observed, whereas a limiting current was observed at the collector electrode. Under low-speed scanning conditions of 0.01 and 0.005 V/s, the anodic and cathodic limiting currents were observed, indicating that the redox cycle was established between the generator and collector electrodes. We considered that the reason for the transition to the sigmoid curve when the scan rate was decreased to 0.01 V/s is as follows. There was sufficient time for the regenerated material ($[FcTAB]^0$) at the collector electrode to travel to the generator electrode, and the consumption and supply of $[FcTAB]^0$ or $[FcTAB]^+$ were balanced. The reported diffusion coefficient (D) of $[FcTAB]^{0/+}$ in aqueous solution is on the order of 10^{-5} cm^2/s.[20,21] By Einstein–Smoluchowski's equation,[22] the approximation equation for diffusion time is given by $t \sim x^2/D$, where t is the elapsed time since diffusion began and x is the mean distance traveled by the diffusing solute in one direction along one axis after t. We thus estimated that the time it takes for $[FcTAB]^{0/+}$ to make a round trip between MGE1 and MGE2 (20 μm × 2 = 40 μm) ranges from 0.2 to 1 s. At a scan rate of 0.005 V/s, where a good redox cycle was observed, it is estimated that $[FcTAB]^{0/+}$ can make a round trip between MGE1 and MGE2 during the time it takes to scan 0.001 V of the measurement step, that is, 0.2 s.

We regarded a current value of 0.6 V, which is the highest potential in the measurement range, as the limiting current for the generator [I_{lim} (g)] and collector [I_{lim} (c)] electrodes. The maximum collection efficiency defined by I_{lim} (c)/I_{lim} (g) reached 97%. We found that I_{lim} (g), I_{lim} (c), and I_{lim} (c)/I_{lim} (g) were almost independent of the scan rate.

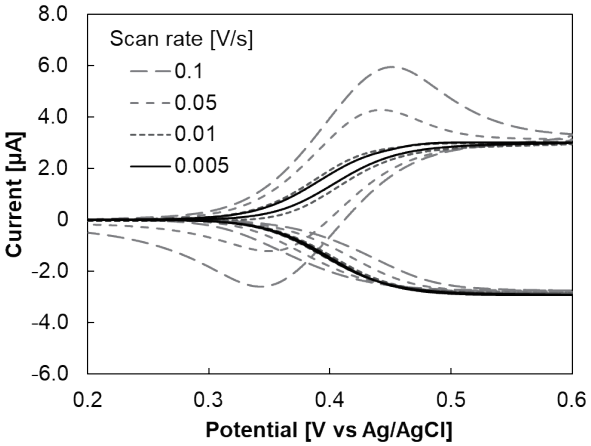

Fig. 5. Dual-mode CV curves with different scan rates obtained with MMGE (1 mM FcTAB in 1 M KCl). The upward and downward currents indicate the oxidation of $[FcTAB]^0$ to $[FcTAB]^+$ and the reduction of $[FcTAB]^+$ to $[FcTAB]^0$ responses, respectively.

$[FcTAB]^0$ moves from the generator to the collector and $[FcTAB]^+$ moves from the collector to the generator between the two bulk electrodes in opposite directions perpendicular to the electrode surface (planar diffusion). In the solution between the two electrodes, the concentrations of both $[FcTAB]^0$ and $[FcTAB]^+$ become constant after a certain period. Therefore, it can be explained that the limiting current was constant without depending on the scan rate. This also describes the reason why such a high collection efficiency can be obtained in spite of the relatively large gap of 20 μm.

4. Conclusions

We have successfully fabricated MMGEs with a gap of 20 μm that enable the measurement of redox cycling on the basal plane by preventing the exposure of highly electrochemically active edges without using a microfabrication process. The typical redox cycling of $[FcTAB]^{0/+}$ was clearly observed by using MMGEs under low-speed scanning conditions of 0.01 and 0.005 V/s. The collection efficiency reached 97% and was almost independent of the scan rate.

The fabrication procedure provided in this study is very simple as we stick the generator and collector fabricated on separate substrates by double-sided tape. It is important to study the relationship between the gap length and the redox cycling characteristics by increasing the number of layers of double-sided tape in the near future. Moreover, it is also possible to modify either or both MGs with functional molecules such as biomolecules or perform doping treatment. It is difficult to fabricate such hetero-electrodes by a microfabrication process applied to the same plane, but our procedure enables us to obtain them. These hetero-MMGEs, which combine one modified MGE with good oxidation properties as a generator electrode and another modified MGE with good reduction properties as a collector electrode, can be used for interesting research such as the observation of redox cycles that cannot be obtained with a homo-MMGE consisting of two MGEs of the same type.

References

1 X. Gan and H. Zhao: Sens. Mater. **27** (2015) 191. https://doi.org/10.18494/SAM.2015.1059
2 S. Z. N. Demon, A. I. Kamisan, N. Abdullah, S. A. M. Noor, O. K. Khim, N. A. M. Kasim, M. Z. A. Yahya, N. A. A. Manaf, A. F. M. Azmi, and N. A. Halim: Sens. Mater. **32** (2020) 759. https://doi.org/10.18494/SAM.2020.2492
3 Y. Ueno: Anal. Sci. **37** (2021) 439. https://doi.org/10.2116/analsci.20SCR08
4 K. Aoki, M. Morita, O. Niwa, and H. Tabei: J. Electroanal. Chem. **256** (1988) 269. https://doi.org/10.1016/0022-0728(88)87003-7
5 O. Niwa, M. Morita, and H. Tabei: Anal. Chem. **62** (1990) 447. https://doi.org/10.1021/ac00204a006
6 O. Niwa, Y. Xu, H. B. Halsall, and W. R. Heineman: Anal. Chem. **65** (1993) 1559. https://doi.org/10.1021/ac00059a013
7 O. Niwa and H. Tabei: Anal. Chem. **66** (1994), 285. https://doi.org/10.1021/ac00074a016
8 M. Morita, O. Niwa, and T. Horiuchi: Electrochim. Acta **42** (1997) 3177. https://doi.org/10.1016/S0013-4686(97)00171-0
9 K. Ito, K. Y. Inoue, T. Ito-Sasaki, M. Ikegawa, S. Takano, K. Ino, and H. Shiku: Micromachines **14** (2023) 327. https://doi.org/10.3390/mi14020327
10 K. Ino, T. Nishijo, Y. Kanno, F. Ozawa, T. Arai, Y. Tatahashi, H. Shiku, and T. Matsue: Electrochemistry **81** (2013) 682. https://doi.org/10.5796/electrochemistry.81.682
11 A. J. Gross and F. Marken: Electroanal. **27** (2015) 1035. https://doi.org/10.1002/elan.201400554

12 K. Ino, M. Şen, H. Shiku, and T. Matsue: Analyst **142** (2017) 4343. https://doi.org/10.1039/C7AN01442B
13 H. S. White and K. McKelvey: Curr. Opin. Electrochem. **7** (2018) 48. https://doi.org/10.1016/j.coelec.2017.10.021
14 K. Ito, K. Y. Inoue, K. Ino, and H. Shiku: Anal. Chem. **94** (2022) 16451. https://doi.org/10.1021/acs.analchem.2c03921
15 Y. Ueno, K. Dendo, Y. Homma, and K. Furukawa: Sens. Mater. **31** (2019) 1157. https://doi.org/10.18494/SAM.2019.2237
16 W. Yuan, Y. Zhou, Y. Li, C. Li, H. Peng, J. Zhang, Z. Liu, L. Dai, and G. Shi: Sci. Rep. **3** (2013) 2248. https://doi.org/10.1038/srep02248
17 A. G. Güell, A. S. Cuharuc, Y.-R. Kim, G. Zhang, S-Y. Tan, N. Ebejer, and P. R. Unwin: ACS Nano **9** (2015) 3558. https://doi.org/10.1021/acsnano.5b00550
18 S. Narafu, Y. Takashima, O. Niwa, T. Yajima, and Y. Ueno: J. Electroanal. Chem. **920** (2022) 116575. https://doi.org/10.1016/j.jelechem.2022.116575
19 Y. Kanno, T. Goto, K. Ino, K. Y. Inoue, Y. Takahashi, H. Shiku, and T. Matsue: Anal. Sci. **30** (2014) 305. https://doi.org/10.2116/analsci.30.305
20 K. Aoki and C. Xiang: J. Phys. Chem. C **111** (2007) 15433. https://doi.org/10.1021/jp071757g
21 N. N. Patel, S. S. Soni, N. Patel, K. Patel, V. K. Patel, D. Sharma, and S. H. Panjabi: ACS Omega **7** (2022) 28974. https://doi.org/10.1021/acsomega.2c02612
22 M-C. Pang, M. Marinescu, H. Wang and G. Offer: Phys. Chem. Chem. Phys. **23** (2021) 27159. https://doi.org/10.1039/D1CP00909E